

RESEARCH

Open Access



# From genes to therapy: a lipid Metabolism-Related genetic risk model predicts HCC outcomes and enhances immunotherapy

Lei Xu<sup>1</sup>, Ting Xiao<sup>2</sup>, Tengfei Chao<sup>3\*</sup>, Huihua Xiong<sup>3\*</sup> and Wei Yao<sup>3\*</sup>

## Abstract

**Background** Hepatocellular Carcinoma (HCC) is related to dysregulated lipid metabolism and immunosuppressive microenvironment. This study developed a genetic risk model using lipid metabolism-related genes to predict survival and immune patterns in HCC patients.

**Methods** Differentially expressed genes (DEGs) related to lipid metabolism were identified in HCC via the TCGA-LIHC dataset. A risk model for survival prediction was constructed via DEGs related to survival. The immune signature associated with the risk model was also evaluated by the CIBERSORT algorithm, tumor immune dysfunction and exclusion algorithm, and single sample gene set enrichment analysis.

**Results** This study identified six lipid metabolism-related genes, *ADH4*, *LCAT*, *CYP2C9*, *CYP17A1*, *LPCAT1*, and *ACACA*, to construct a lipid metabolism-related gene risk model that can divide HCC patients into low- and high-risk groups. Internal and external validation verified that the risk model could be a signature that could effectively predict HCC patient prognosis. High-risk patients showed disrupted immune cell profiles, reduced tumor-killing capacity, and increased expression of immune checkpoint genes. However, they responded more favorably to immune checkpoint inhibitor (ICB) therapy. The top ten hub genes related to the risk model were associated with tumor progression and deteriorating prognosis. In vitro experiments verified that the downregulation of the top 1 hub gene *CDK1* was correlated to the HCC cell proliferation.

**Conclusion** The risk model constructed using lipid metabolism-related genes could effectively predict prognosis and was related to the immunosuppressive microenvironment and ICB immunotherapy. The hub genes related to the risk model were potential therapeutic targets.

**Keywords** Hepatocellular carcinoma, Lipid metabolism, Risk model, Survival prediction, Tumor immunity, Immune checkpoint Blockade, Bioinformatics

\*Correspondence:

Tengfei Chao  
turnface@126.com  
Huihua Xiong  
lizaabear@tjh.tjmu.edu.cn  
Wei Yao  
yw13557@tjh.tjmu.edu.cn

<sup>1</sup>Department of Pediatrics, Tongji Hospital, Tongji Medical College, Huazhong University of Science and Technology, Wuhan, Hubei 430030, China

<sup>2</sup>Department of Ultrasonography, Tongji Hospital, Tongji Medical College, Huazhong University of Science and Technology, Wuhan, Hubei 430030, China

<sup>3</sup>Department of Oncology, Tongji Hospital, Tongji Medical College, Huazhong University of Science and Technology, Wuhan, Hubei 430030, China



© The Author(s) 2025. **Open Access** This article is licensed under a Creative Commons Attribution-NonCommercial-NoDerivatives 4.0 International License, which permits any non-commercial use, sharing, distribution and reproduction in any medium or format, as long as you give appropriate credit to the original author(s) and the source, provide a link to the Creative Commons licence, and indicate if you modified the licensed material. You do not have permission under this licence to share adapted material derived from this article or parts of it. The images or other third party material in this article are included in the article's Creative Commons licence, unless indicated otherwise in a credit line to the material. If material is not included in the article's Creative Commons licence and your intended use is not permitted by statutory regulation or exceeds the permitted use, you will need to obtain permission directly from the copyright holder. To view a copy of this licence, visit <http://creativecommons.org/licenses/by-nc-nd/4.0/>.

## Introduction

Hepatocellular carcinoma (HCC) remains a formidable global health challenge, ranking as the sixth most prevalent malignancy and the second leading cause of cancer-related mortality worldwide [1]. In the early stage, most HCC patients are asymptomatic, which results in late diagnosis, and only approximately one-third of cases have an opportunity for curative treatments [1, 2]. Tumor recurrence occurs in 70% of HCC patients receiving radical surgery within 5 years [1, 2].

No effective treatments were available for patients with advanced-stage HCC before 2008 [2]. A comprehensive understanding of molecular mechanisms of tumor initiation and progression has led to the introduction of targeted therapy and immunotherapy and improved outcomes for HCC patients [3–7]. For example, sorafenib [8], lenvatinib [9], cabozantinib [10], ramucirumab [11], and regorafenib [12] have been authorized as the first/second-line systemic drugs for HCC treatment by The FDA. When compared to placebo, sorafenib led to an increase in the median survival time by nearly 3 months [1, 8]. Although these therapies improve short-term outcomes, HCC patients still face poor long-term survival, highlighting the need for continued research.

Emerging evidence highlights metabolic reprogramming as a fundamental driver of oncogenesis and tumor progression [13]. The liver is a vital organ for the metabolism of lipids, and dysregulated lipid metabolism, such as metabolic-associated fatty liver disease (MAFLD), significantly increases the risk of HCC [14]. Lipids fuel tumor growth by acting as energy sources and signaling molecules. They also help create an immune-suppressive environment that aids cancer progression [15–18]. Previous studies have confirmed that lipid metabolism-related genes were closely related to HCC patient prognosis, and these genes as therapeutic targets benefited HCC patients [19, 20]. Thus, lipid metabolism genes can be potential prognostic biomarkers and therapeutic targets and need further investigation for HCC patients.

Capitalizing on the well-established linkage between dysregulated lipid metabolism and HCC pathogenesis, we developed an innovative prognostic model with three

key advances. First, unlike traditional gene-based predictions, our model integrates tumor immune environment data. This lipid metabolism-related signature uniquely reveals immune differences across risk groups, including immune cell infiltration, tumor-killing capacity, and checkpoint protein levels. Second, it predicts patient responses to immunotherapy (ICB), making it both a prognostic tool and treatment guide. Third, we identified CDK1 as the core hub gene in this lipid network. Our analysis shows CDK1 drives HCC proliferation, offering new treatment targets that link metabolism and immunity.

## Materials and methods

### Data download

The clinical features of the HCC patients and corresponding mRNA expression patterns were obtained from the TCGA-LIHC dataset and delineated as the training group. Besides, the clinical traits of HCC patients and corresponding mRNA expression profiles were available from the ICGC (LIRI-JP) data portal and delineated as the testing group. The clinical characteristics between training and testing group were listed in Table 1. scRNA-seq data (GSE223204) were downloaded from The Gene Expression Omnibus, which included single cell RNA data of tumor and normal tissue in HCC patient. The lipid metabolism-related genes were obtained from Gene Set Enrichment Analysis (GSEA) dataset.

### Differential gene expression analysis

False discovery rate  $< 0.05$  and  $|\text{Log}_2 \text{fold change}| > 0.585$  were the thresholds to determine differentially expressed genes (DEGs). Based on the “edgeR” (version 3.36.0) R package [21], the DEGs related to lipid metabolism between normal and tumor tissues were screened using the mRNA expression profiles from the training group.

### Development of a risk model via DEGs related to lipid metabolism

The “survival” (version 3.3.1) R package identified the prognostic genes from the differentially expressed genes related to lipid metabolism by univariate regression analysis and logistic LASSO regression analysis. We chose LASSO regression for feature selection because it effectively handles high-dimensional data. This machine learning technique employs L1 regularization to mitigate overfitting while simultaneously performing automated feature shrinkage and dimensionality reduction. The algorithm’s inherent capacity to maintain optimal predictive accuracy while generating parsimonious models makes it particularly advantageous for clinical translation, where model interpretability and operational feasibility are critical considerations. Then, a risk model was developed using the identified prognostic genes, and

**Table 1** Clinical characteristics between training and testing group

Items	TCGA (n=365)	ICGC (n=232)	p Value
Age (years)	69.78 ± 30.87	67.72 ± 10.10	0.1018
Sex (male)	246	171	0.1015
Survival time (days)	811.9 ± 725.8171	811.9 ± 417.7	0.9998
<b>Tumor stage</b>			
I	170	36	
II	85	105	
III	74	71	
IV	4	19	< 0.0001

each HCC patient was assigned a risk score (RS) determined by the following equation:

$$RS = \sum_{m=1}^i Coef_m \times exp_m$$

where “*i*” signifies the number of lipid metabolism-related genes, “*Coef<sub>m</sub>*” represents the logistic LASSO regression coefficient of gene *m*, and “*exp<sub>m</sub>*” represents the mRNA expression level of gene *m*. HCC patients were classified into high- and low-risk groups via the median RS, with the high-risk group having a higher RS.

#### Validation of the risk model related to lipid metabolism

The predictive value of the risk model was internally validated by the training group and externally validated by the testing group. First, principal component analysis (PCA) was performed to visualize and compare the predictive ability of the risk model by the “scatterplot3d” (version: 0.3–41) R package. Second, the risk plot demonstrated the differences in the survival between the low- and high-risk groups by the “heatmap” (version: 1.0.12) R package. Third, Kaplan-Meier survival curves determined the differences in overall survival (OS) between the low- and high-risk groups via the “survminer” (version: 0.4.9) and “survival” (version: 3.3-1) R packages. Four, the area under the curve (AUC) of the receiver operating characteristic (ROC) curves for the survival prediction were determined from the “survivalROC” (version:1.0.3) R package. Finally, The C-index evaluates the concordance between predicted and observed survival outcomes within each cohort independently using the “survcomp” (version: 1.44.1) R package [22], reflecting the model’s ability to rank patients by risk.

#### Nomogram construction and validation

Nomograms are commonly used tools for predicting survival in oncology research [23, 24]. In this study, a nomogram was developed by integrating the lipid metabolism-related gene risk model with the clinical characteristics using the “rms” (version: 6.3-0), “foreign” (version: 0.8–82), and “survival” (version: 3.3-1) R packages. The predictive prognostic value of the nomogram was estimated by the AUC of the ROC and C-index. In addition, calibration curves were used to assess the consistency between the observed and predicted survival rates.

#### Investigation of the immune signature related to the risk model

In this study, CIBERSORT, a flexible computational algorithm for quantifying cell proportions via gene expression profiles, was used for estimating the proportion of 22 types of immune cell subclusters for each HCC patient [25, 26]. The normalized enrichment scores of

13 different immune functions were determined by the single sample GSEA (ssGSEA) by “GSEABase” (version:1.58) and “GSVA” (version: 1.44) R packages [27]. The potential response to anti-PD1 and anti-CTLA4 immunotherapies was estimated by the Tumor Immune Dysfunction and Exclusion (TIDE) score, and a lower TIDE prediction score indicated a better response [28].

#### Identification of the hub genes of the risk model

The DEGs between high- and low-risk groups were determined by the “edgeR” (version 3.36.0) R package. Based on DEGs, The STRING online database with an interaction confidence score  $\geq 0.9$  was used to build protein-protein interaction (PPI) network. Then, the PPI network was visualized by Cytoscape software, and the hub genes were obtained by the “CytoHubba” plug-in using the degree method.

#### Functional enrichment analyses

Biological activities and signaling pathways of the genes were determined by GO and KEGG enrichment analyses based on the “org.Hs.eg.db” (version 3.14.0), “enrichplot” (version 1.14.2), and “clusterProfiler” (version 4.2.2) R packages.

#### scRNA-seq data analysis

The “Seurat” (version 4.4.0) R package was used to analyze the scRNA-seq data in the following ways: (1) Using the “CreateSeuratobject” function, the scRNA-seq data were read and transformed into Seurat objects. Genes expressed in less than three cells were eliminated, whereas cells with 200–4000 genes and a mitochondrial gene percentage of less than 20% were allowed. The R package “scDblFinder” (version 1.16.0) was utilized to detect and eliminate doublets/multiplts. The R package “ccRemover” (version 1.0.4) was utilized to detect and eliminate cell-cycle effects. (2) Following quality control, Seurat objects were combined using the “FindIntegrationAnchors” and “IntegrateData” functions, then normalized using the “NormalizeData” function. (4) The “FindVariableFeatures” program was used to determine the top 2000 highly variable genes. Principal component analysis (PCA) and uniform manifold approximation and projection (UMAP) analysis were utilized to determine cell clusters using these highly variable genes. (5) Each cell cluster was annotated via DEGs and specific marker genes. Variations in lipid metabolism pathway were assessed using the “GSVA” R package via Gene Set Variation Analysis (GSVA) 29, with the “methods” parameter configured to “ssGSEA” and all other parameters set to default.

### Cell transfection

Small interfering RNAs (siRNAs) were used to specifically knock down *CDK1* in the Huh7 cells. The sequences of the siRNAs are shown in Table 2.

### Quantitative real-time PCR (qRT-PCR) and Western blotting

The protein and RNA expression level of *CDK1* were detected by Western Blotting and qRT-PCR analysis based on the standard protocols. The primary and secondary antibodies for western blotting are provided in Table 3, and the primers for qRT-PCR are given in Table 4.

### 5-Ethynyl-2'-Deoxyuridine (EdU) assay

The knockdown of the *CDK1* gene in HCC cells and their corresponding control cells were incubated in a culture plate at a rate of  $1 \times 10^5$  cells per well for 24 h. The EdU assay was performed using the EdU Assay Kit (Absin, China) as per the manufacturer's instructions. Quantitative analysis of EdU-positive cells was performed using ImageJ software. Fine independent biological replicates were analyzed. Statistical significance was determined using a two-tailed Student's t-test.

## Results

### Construction of the lipid metabolism-related gene risk model

786 genes related to lipid metabolism were selected from the GSEA database (Table. S1). Then, 70 DEGs related to lipid metabolism between HCC tumors and normal tissues were identified in the training group, consisting of 36 downregulated and 34 upregulated genes in tumor tissues (Fig. 1A). The univariate regression analysis confirmed 37 lipid metabolism genes associated with the survival of HCC patients (Fig. 1B). Finally, six lipid metabolism genes, namely, *ADH4*, *LCAT*, *CYP2C9*, *CYP17A1*, *LPCAT1*, and *ACACA* were identified by the logistic LASSO regression analysis (Fig. 1C). HCC patients with high *ACACA* and *LPCAT1* expression had worse survival probability. HCC patients with increased expression of *ADH4*, *LCAT*, *CYP2C9*, and *CYP17A1* had better survival probability (Fig. 1D). scRNA-seq analysis identified cell-type-specific lipid metabolism patterns in HCC (Fig. 1E-G). Hepatocytes predominantly expressed *ADH4*, *LCAT*, *CYP2C9*, *ACACA*, and *CYP17A1*, showing strong cholesterol and triglyceride biosynthesis (Fig. 1F-G). Neutrophils enriched with *LPCAT1* exhibited marked cholesterol import and triglyceride breakdown (Fig. 1F-G). Monocytes demonstrated active fatty acid uptake (Fig. 1G). Stromal cells displayed dual cholesterol import and export, suggesting extracellular lipid remodeling (Fig. 1G). These compartmentalized metabolic activities reveal specialized lipid handling across HCC microenvironment components.

**Table 2** siRNA for CDK1

Gene	Name	SS sequence	AS sequence
CDK1	si-1	GGUUAGUUCUAGAUCACUAAU	UAGUGAUCUA-GAACUAACCAA
	si-2	GGAAUUAUGACAGAAGGUUAAU	UAACCUUCUGU-CAUAUCCUA
	si-3	GAAGCUAAAUACUACACUAGU	UAGUGUAGUAU-UUAGCUUCUU

**Table 3** Antibodies of the target genes

Gene	Primary antibody	Secondary antibody
CDK1	A0220 (Abclonal)	Goat anti-rabbit IgG H&L (HRP) (abs20002)
B-ACTIN	Abs119600 (Absin)	Goat anti-rabbit IgG H&L (HRP) (abs20002)

**Table 4** Primers for the target genes

Gene	Forward primer	Reverse primer
CDK1	AACTACAGGTCAAGTGGTAGCCATG	TCCATGTACTGAC-CAGGAGGGATAG
B-ACTIN	CAGATGTGGATCAGCAAGCAGGAG	AAGCCATGCCAAT-GAGACTGAGAAG

Further, the gene risk model was constructed by the six genes to predict the prognosis in HCC patients, and each patient was assigned an RS (Table. S2). The equation used for calculating RS is provided in the Material and Methods section. HCC patients with high RS had higher histologic neoplasm grade, advanced T stage, and advanced TNM stage than patients with low RS (Fig. 1H). Therefore, the lipid metabolism-related gene risk model was significantly associated with tumor progression.

Thorsson et al. identified six immune subtypes (C1 to C6) based on the immunogenomic analyses of 33 cancer types from the TCGA database [29]. HCC tumor samples were divided into four immune subtypes (C1 to C4), including wounding healing, IFN- $\gamma$  dominant, inflammatory, and lymphocyte depleted. This study confirmed the statistical differences in RS among the four immune subtypes. HCC tumor samples belonging to the C1 (wounding healing) immune subtype had the highest RS than other samples, while samples belonging to C3 (inflammatory) had the lowest RS (Fig. 1I). Hence, it can be stated that the risk model was also associated with tumor immunity.

### Validation of the risk model for prognostic prediction

The HCC samples from the TCGA-LIHC dataset were defined as the training group for internal validation of the six-gene risk model. All the HCC patients were classified into low- or high-risk groups via the median of RS, and patients in the low-risk group had a lower RS (Table. S2). The accuracy of the six-gene risk model in predicting the prognosis in different populations was determined by the HCC samples from the ICGC dataset which was defined

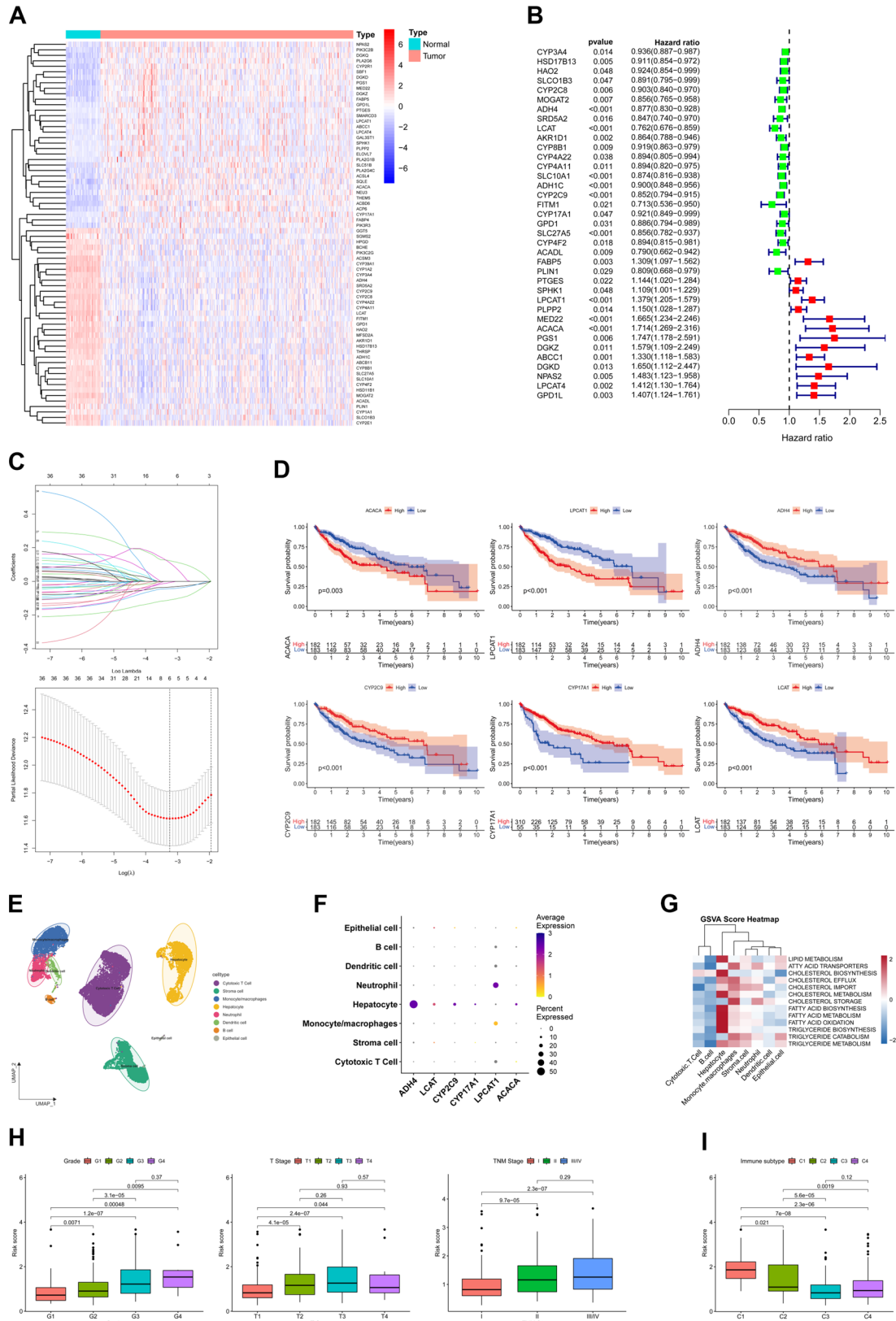


**Fig. 1** (See legend on next page.)

(See figure on previous page.)

**Fig. 1** Construction of the lipid metabolism-related gene risk model. **(A)** The Heatmap plot shows DEGs between normal and tumor tissues in HCC. **(B)** The Forest plot shows 37 survival-related lipid metabolism genes identified by the univariate regression analysis. **(C)** Six out of 37 prognostic genes were selected by the LASSO Cox regression model. **(D)** Kaplan-Meier curves comparing the groups with different expression levels of 6 genes in HCC patients. **(E)** A total of 16,649 quality controlled single cells derived from tumor and normal tissues in HCC were divided into 8 cell-types based on scRNA-seq analysis. **(F)** scRNA-seq analysis showed the expression of the six selected prognostic genes in each cell-type. **(G)** GSEA evaluated lipid metabolism pathway enriched in each cell type. **(H)** The box plot shows the relationship between the genetic risk model and the clinical features, including histologic neoplasm grade, T stage, and TNM stage. **(I)** The box plot shows the mean RSs in different immune subtypes

as testing group for the external validation. The HCC patients from the testing group were also assigned RS based on the Cox proportional-hazards model and were divided into low- or high-risk groups using the median of RS (Table. S3).

PCA analysis confirmed that RS could indicate the distinctive features of HCC patients in terms of distinct lipid metabolism-related gene expression (Fig. 2A and Fig. S1A). The risk plot demonstrated that patients in the low-risk group had better survival chances and survival times (Fig. 2B and Fig. S1B). Kaplan-Meier survival analysis substantiated that HCC patients in the low-risk group had a higher OS probability (Fig. 2C and Fig. S1C). The univariate (Fig. 2D and Fig. S1D) and multivariate (Fig. 2E and Fig. S1E) Cox regression analysis confirmed that the RS was an independent prognosis factor. The AUCs of the 1-year, 2-year, and 3-year ROC curves were 0.749, 0.722, and 0.704 for the training group (Fig. 2F), respectively, and 0.761, 0.711, and 0.720 for the testing group, respectively (Fig. S1F). In addition, ROC curves indicated that the risk model had better survival diagnostic performance than the clinical parameters, including gender, age, histologic neoplasm grade, and TNM stage (Fig. 2G and Fig. S1G). The C-index was 0.693 ( $P < 0.001$ ) for the training group and 0.721 ( $P < 0.001$ ) and for the testing group (Table 5). Thus, both the internal and external validation confirmed that the lipid metabolism-related gene risk model could accurately predict HCC patient prognosis.

#### Development of a nomogram integrating risk model with the clinical parameters for prognosis prediction

Further, in this study, the clinical parameters were integrated with RS to build a nomogram for the prediction of HCC patient prognosis (Fig. 3A). The univariate (Fig. 3B) and multivariate (Fig. 3C) Cox regression analyses showed that the nomogram was an independent prognosis factor. The calibration curve exhibited an excellent consistency between the observed survival probability and that predicted by the nomogram (Fig. 3D). Besides, the AUCs of the ROC curves for the 1-year, 3-year, and 5-year survival prediction were 0.767, 0.704, and 0.697, respectively, which also indicated that the nomogram showed a better survival diagnostic performance than RS and clinical parameters (Fig. 3E). Thus, a nomogram integrating the clinical parameters with gene signature is a better prognostic signature.

#### Investigation of the immune signature related to risk mode

The CIBERSORT estimated the proportions of 22 immune cell subclusters for each HCC patient (Fig. 4A). HCC patients in the high-risk group had a higher average percentage of follicular helper T cells, M0 macrophages, memory B cells, and neutrophils but a lower average percentage of M2 macrophages, naïve B cells, and  $\gamma\delta$  T cells when compared to the low-risk group (Fig. 4B). Further, ssGSEA correlation analysis indicated that antitumor-related immune functions, including cytolytic activity, type I and II IFN response were weakened in the high-risk group (Fig. 4C). Meanwhile, the high-risk group lowly expressed the cytotoxic effectors GZMK and FAS1 (Fig. 4D).

As the ICGs regulated antitumor immunity, the association between lipid metabolism-related gene risk model and ICGs, including 20 stimulatory ICGs, 21 inhibitory ICGs, and 27 two-sided ICGs reported by the previous studies (Table. S4) [30], was investigated. The high-risk group differentially expressed nearly half of the inhibitory ICGs (9 upregulated and 1 downregulated), one-third of the stimulatory ICGs (7 upregulated), and a quarter of two-sided ICGs (5 upregulated and 1 downregulated) (Fig. 4E and Fig. S2A-B). TIDE [28] was performed to predict ICB response, which highlighted that the high-risk group presented a lower mean TIDE score (Fig. 4F). This indicates anti-CTLA4 and anti-PD1 therapies may be more effective for HCC patients with high RS.

#### Analysis of DEGs between low- and high-risk groups

The DEGs between the low and the high-risk groups were further investigated to elucidate the potential pathways by which lipid metabolism-related genes regulate prognosis and tumor immunity. The high-risk group downregulated 132 genes and upregulated 315 genes (Fig. 5A and Table. S5). Based on STRING online database, the DEGs were analyzed to construct a PPI network (Fig. 5B). Then, the PPI network was visualized by the Cytospace software (Fig. S3A), which further helped us to identify that *CDK1*, *CDC20*, *BUB1*, *CCNB1*, *CCNB2*, *AURKB*, *TOP2A*, *BUB1B*, *KIF11*, and *ASPM* were the top 10 hub genes (Fig. 5C and Table. S6). In this study, the patients highly expressed top 10 hub genes had worse OS (Fig. 5D and Fig. S3B). Besides, the enhanced expression levels of the top 10 hub genes were related to higher histologic neoplasm grade (Fig. 5E), advanced T stage (Fig. S3C), and advanced TNM stage (and Fig. S3D). Moreover,

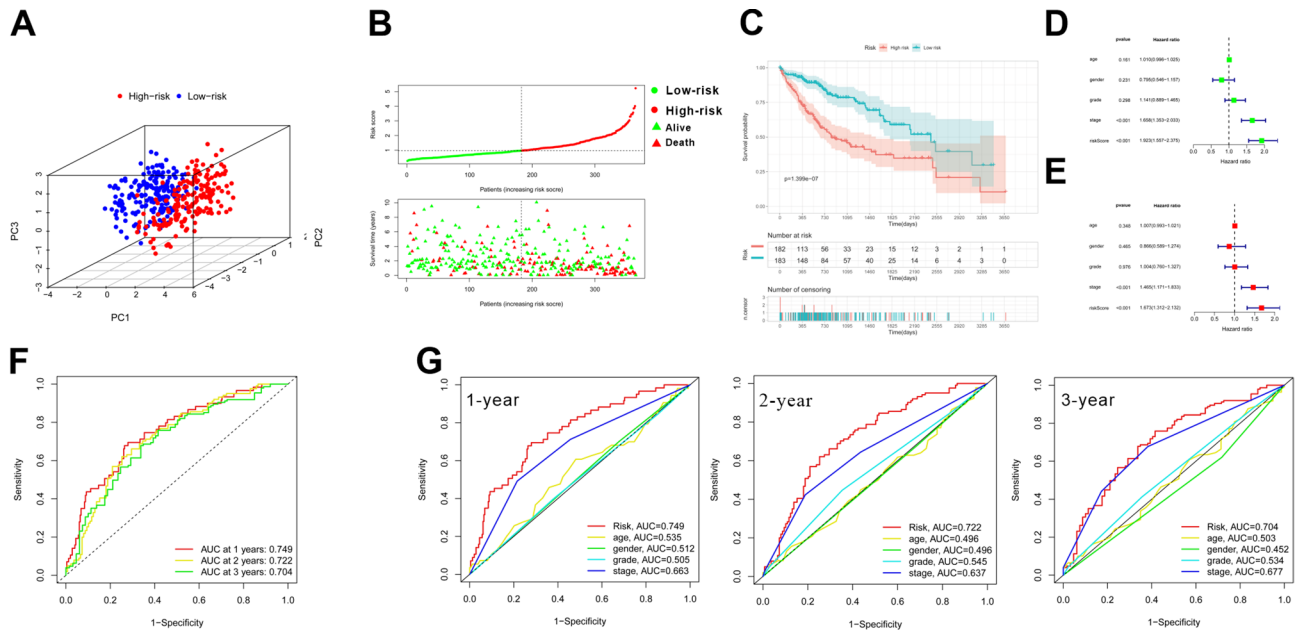


**Fig. 2** Internal validation of the risk model via TCGA dataset. **(A)** PCA plot shows expression profiles of six prognostic genes in different risk groups. **(B)** The risk plot shows the RS for each HCC patient and indicates that patients with high RS have worse survival times and survival rates. **(C)** Kaplan-Meier curves confirmed that the high-risk group had a lower survival probability. **(D-E)** Univariate Cox regression analysis **(D)** and multivariate Cox regression analysis **(E)** confirmed that RS could be an independent prognosis factor in HCC. **(F)** ROC curve indicated that the risk model could accurately predict HCC patient prognosis. **(G)** The ROC curve of time survival indicated that the risk model had better prognostic prediction performance than the clinical parameters

**Table 5** The C-index for training and testing dataset

Dataset	C-index (95%CI)	P Value
TCGA	0.693 (0.645–0.742)	<0.001
ICGC	0.721 (0.639–0.804)	<0.001

enhanced expression of the top 10 hub genes were related to the high average proportions of memory B cells, M0 macrophages, resting dendritic cells, activated memory CD4 T cells, follicular helper T cells, and Tregs but to the low average proportions of resting  $\gamma\delta$  T cells, naïve B cells, NK cells, and M2 macrophages, which was almost consistent with the findings from the lipid metabolism-related gene risk model (Fig. S3E). Thus, it can be stated that the top 10 hub genes may be the key genes related to tumor progression, deteriorating prognosis, and tumor immunity.

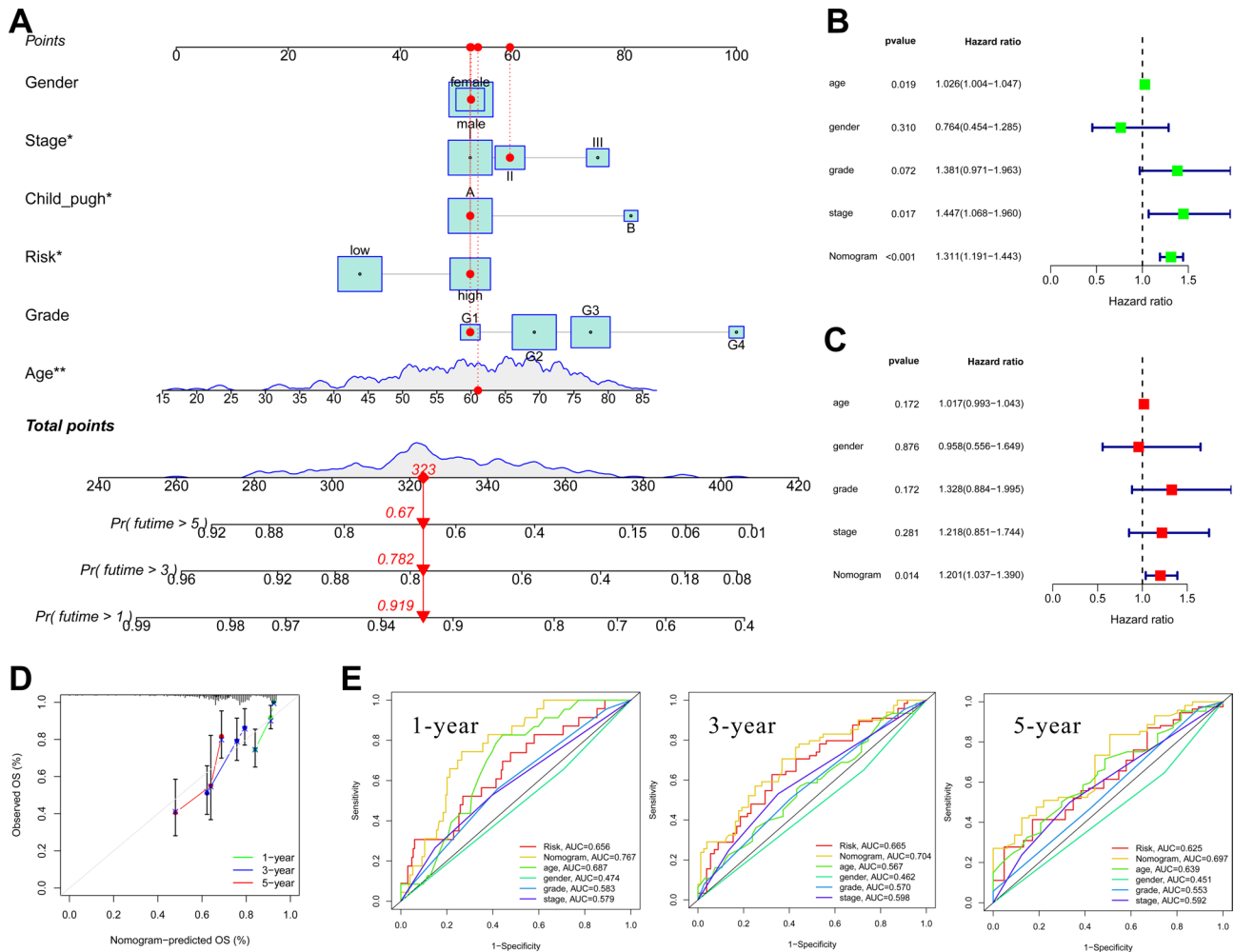
Further, the underlying biological processes were elucidated by the GO and KEGG enrichment analyses. GO enrichment analysis showed that nuclear division, chromosome segregation, mitotic nuclear division, sister chromatid segregation, and mitotic sister chromatid segregation were the top 5 biological processes; spindle, chromosomal region, chromosome (centromeric region), condensed chromosome (centromeric region), and kinetochore were the top 5 cellular components; and microtubule binding, organic acid transmembrane transporter activity, xenobiotic transmembrane transporter activity, steroid hydroxylase activity, and DNA replication origin binding were the top 5 molecular functions (Fig. 5F and

Fig. S3F). Similarly, KEGG pathway enrichment analysis indicated that cell cycle, oocyte meiosis, bile secretion, progesterone-mediated oocyte maturation, and p53 signaling pathway were the top 5 pathways (Fig. 5G and Fig. S3G).

**The expression of prognostic genes related to lipid metabolism and the top 10 hub genes in HCC.**

Both the testing and training groups have confirmed that RNAs of the prognostic genes, namely, *ACACA* and *LPCAT1*, were expressed at high levels in the tumor tissues and high-risk group compared to normal tissue and low-risk group, respectively (Fig. 6A-B and Fig. S4A-B). On the contrary, *ADH4*, *LCAT*, and *CYP2C9* were lowly expressed in tumor tissue and high-risk group (Fig. 6A-B and Fig. S4A-B). *CYP17A1* was expressed at high levels in tumor tissue and the low-risk group (Fig. S4A-B). The Human Protein Atlas (HPA) also confirmed that protein expression and showed *ACACA* and *LPCAT1* were significantly higher in HCC tumor tissues and *ADH4* and *CYP2C9* were considerably higher in normal liver tissues (Fig. 6C).

The testing and training groups confirmed that the RNAs of the top 10 hub genes were highly expressed in tumor tissue and high-risk group compared to normal liver tissue and low-risk groups (Fig. 6D-E and Fig. S4C-D). The HPA database also confirmed that the protein expression of the hub genes were higher in tumor tissues, except for *BUB1*, *BUB1B*, and *ASPM* as the



**Fig. 3** Construction and validation of nomogram. **(A)** A nomogram integrating clinical parameters with RS for prognosis prediction. **(B-C)** Univariate Cox regression analysis **(B)** and multivariate Cox regression analysis **(C)** confirmed that the nomogram was an independent prognosis factor. **(D)** Calibration plots predict the survival probability for HCC patients. The y-axis shows the actual survival probability, while the x-axis shows the predicted survival probability. **(E)** ROC curves indicated that the nomogram had better prognostic prediction performance than the clinical parameters and lipid metabolism-related gene risk model

immunohistochemical information of these three could not be found in the HPA database (Fig. 6F and Fig. S4E).

**Identification of the top 1 hub gene CDK1 in vitro experiments**

12 pairs of matched HCC normal and tumor tissues were tested by qRT-PCR and western blotting experiments, which indicated that the RNA and protein expression levels of *CDK1* were higher in tumor tissues (Fig. 7A and B). As the functional enrichment analysis indicated that the biological processes in the high-risk group were mainly enriched in cell proliferation, the biological functions of the top 1 hub gene *CDK1* were further confirmed in vitro experiments. *CDK1* knockdown in Huh7 cells by siRNAs was confirmed by qRT-PCR (Fig. 7C) and western blotting experiments (Fig. 7D). The EdU assay confirmed that downregulation of *CDK1* led to a decrease in HCC cell

proliferation (Fig. 7E), which was in agreement with the functional enrichment analyses.

**Discussion**

HCC is a common and one of the most lethal tumors characterized by late diagnosis, early recurrence, metastasis, and poor diagnosis [31-33]. It is challenging to treat this disease as the treatment options are limited. During the past decade, the short-term outcome of HCC patients has been improved by immunotherapy and targeted therapy, but the long-term prognosis still needs further development [6, 7]. Lipids, as signaling molecules and energy sources, support cancer progression and immunosuppressive microenvironment [34, 35]. The liver is a central organ for lipid metabolism, and the dysregulation of lipid metabolism is the major risk factor for HCC [36].

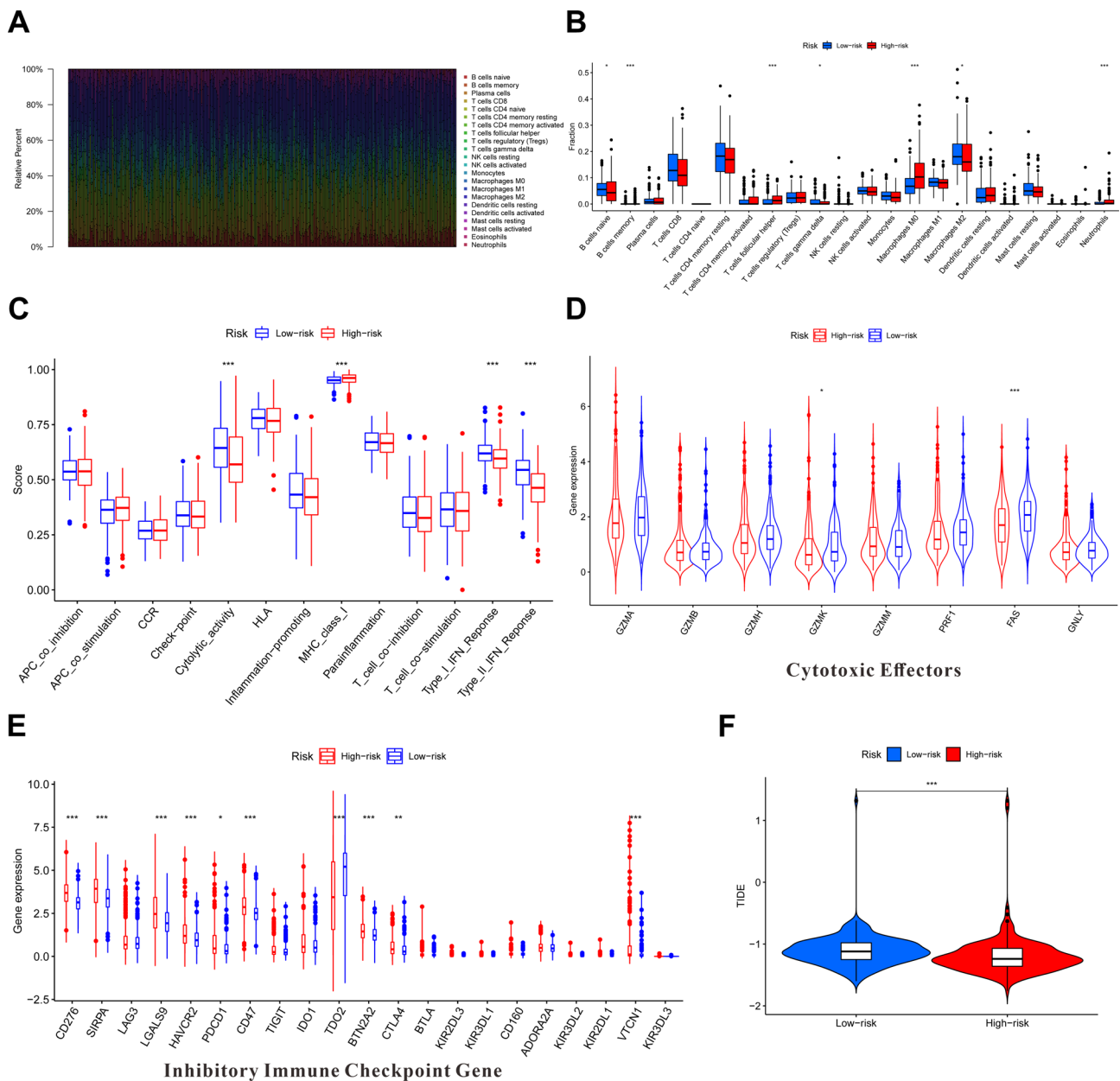


**Fig. 4** Immune signatures related to risk model. **(A)** CIBERSORT calculated the relative proportions of immunocytes for each HCC patient in the training group. **(B)** Mean relative proportions of immunocytes between the low- and high-risk groups. **(C)** ssGSEA calculated the normalized enrichment scores for 13 different immune function pathways between the two groups. **(D)** Expression of cytotoxic effectors between two groups. **(E)** mRNA expression of inhibitory ICGs between two groups. **(F)** TIDE scores of the low- and high-risk groups. \*:  $P < 0.05$ ; \*\*:  $P < 0.01$ ; \*\*\*:  $P < 0.001$ ; \*\*\*\*:  $P < 0.0001$

Lipid metabolism-related genes are potential prognostic biomarkers and therapeutic targets in HCC patients [37].

In this study, Analysis of TCGA data revealed six differentially expressed genes (DEGs) - *ADH4*, *LCAT*, *CYP2C9*, *CYP17A1*, *LPCAT1*, and *ACACA* - associated with both lipid metabolism and survival outcomes in hepatocellular carcinoma (HCC). Single-cell RNA sequencing demonstrated predominant expression of these survival-related lipid metabolism genes in hepatocytes. Multi-dataset validation (ICGC, TCGA, HPA) showed distinct expression

patterns: *ADH4* and *CYP2C9* exhibited significantly reduced RNA/protein levels in tumor tissues compared to normal liver, while *ACACA* and *LPCAT1* displayed marked overexpression in malignant lesions.

Clinically, reduced expression of *ADH4*, *LCAT*, *CYP2C9*, and *CYP17A1* correlated with poorer patient survival, whereas lower *ACACA* and *LPCAT1* levels paradoxically associated with improved prognosis. While existing literature has established the tumorigenic roles

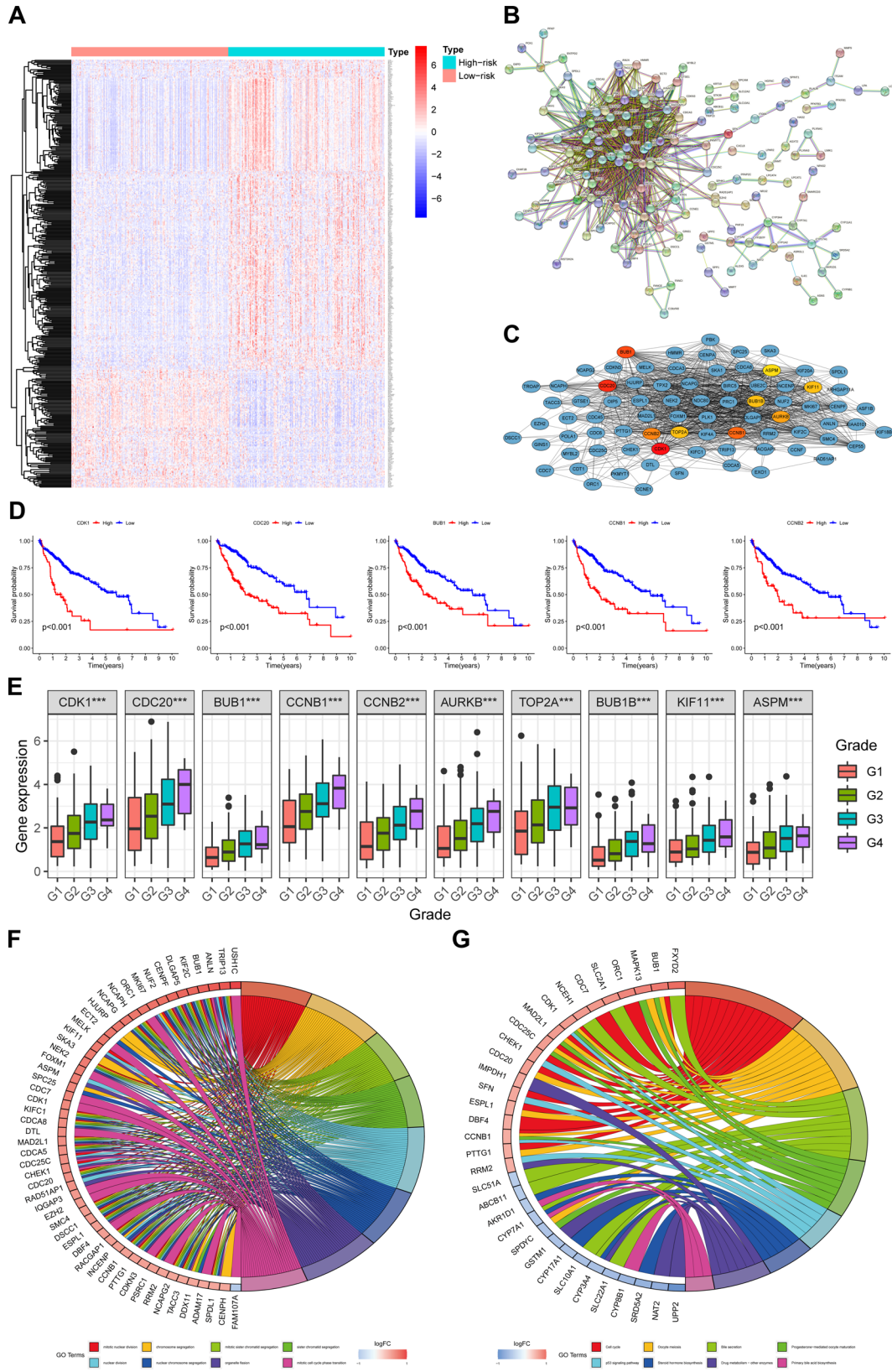


Fig. 5 (See legend on next page.)

(See figure on previous page.)

**Fig. 5** Analysis of DEGs between low-risk and high-risk groups. **(A)** The Heatmap plot shows DEGs between two groups. **(B)** The PPI network was constructed based on the DEGs. **(C)** The top ten hub genes marked in red were determined from the PPI network by Cytoscape software. **(D)** Kaplan-Meier curves confirmed that the high expression of the top ten hub genes in HCC patients indicated worse survival probability. **(E)** High expression levels of the top ten hub genes were associated with high histologic neoplasm grade. **(F)** GO enrichment analysis for the DEGs. **(G)** KEGG enrichment analysis for the DEGs

\*\*\*:  $P < 0.001$

of *LCAT*, *ACACA* and *ADH4* in HCC, recent mechanistic studies provide new insights:

Xu et al. identified *LCAT* as a tumor suppressor through dual metabolic regulation. Their work revealed that *LCAT* inhibits triglyceride hydrolysis by disrupting *CAV1-PRKACA* interactions while simultaneously suppressing fatty acid oxidation via *CPT1A* degradation, thereby depriving tumor cells of critical metabolic substrates. Clinically, *LCAT* deficiency correlates with aggressive tumor behavior and reduced therapeutic response to lenvatinib. Notably, pharmacological inhibition of fatty acid oxidation restored treatment sensitivity in *LCAT*-deficient HCC models [38]. Liu et al. demonstrated that trichostatin A (TSA) can attenuate HCC progression and reduced hepatic lipid accumulation. Mechanistically, TSA was found to restore *c-Myc* suppressed *ADH4* expression through *AKT/mTOR* pathway inhibition. This metabolic reprogramming corrected *c-Myc* induced *NAD<sup>+</sup>/NADH* imbalance and ATP depletion, positioning *ADH4* as a crucial nexus between oncogenic signaling and metabolic homeostasis in HCC [39]. Peng et al. characterized *ACACA* as a pivotal fatty acid synthase in HCC pathogenesis. *FASRL* binding to *ACACA* increases fatty acid synthesis and lipid accumulation to mechanistically exacerbate HCC [40].

A genetic risk model was constructed by integrating six lipid metabolism-related genes *ADH4*, *LCAT*, *CYP2C9*, *CYP17A1*, *LPCAT1*, and *ACACA*. Notably, HCC patients with high RS showed higher histologic neoplasm grade, advanced T stage, and advanced TNM stage. Both the risk plot and Kaplan-Meier survival analysis confirmed that HCC patients with high RS had a worse OS probability. The univariate and multivariate Cox regression analyses confirmed that RS was an independent prognosis factor in HCC patients. Moreover, the ROC curve confirmed that the risk model could accurately predict HCC patient prognosis and showed better survival diagnostic performance compared to clinical parameters, including age, gender, histologic neoplasm grade, and stage. TNM staging system was proposed in 1953 as a common language for solid tumor prognosis [41], and recently served as the holy grail of prognostic models in cancer research [23]. However, the present study proved that the gene risk model based on prognostic genes related to lipid metabolism had better prognostic prediction performance than that based on TNM staging in HCC patients. Thus, the lipid metabolism-related gene risk model consisting of

*ADH4*, *LCAT*, *CYP2C9*, *CYP17A1*, *LPCAT1*, and *ACACA* showed prognostic significance for HCC patients.

Medical nomograms based on the clinical and biological parameters were used to construct a statistical prognostic model for calculating the probability of a clinical event for a particular individual, for example, cancer recurrence or death [23, 24]. A nomogram model integrating RS and clinical parameters was constructed for predicting personalized HCC patient prognosis in this study. The ROC curve confirmed that the nomogram had better prognostic prediction performance compared with RS and traditional clinical parameters. Thus, the present study provides an improvised model which may be a valuable and effective tool for predicting HCC patient prognosis.

This study indicated that the lipid metabolism-related gene risk model was significantly associated with tumor progression and prognosis. In addition to lipids being a backup energy source to make up for energy shortages, they are involved in forming biological membranes, serving as substrates for biomass production, and activating intricate signaling pathways, which directly contribute to malignant transformation, proliferation, and migration in cancer cells [42, 43]. KEGG and GO enrichment analyses also confirmed that the upregulated DEGs in high-risk groups were strongly associated with cell division, proliferation, and survival. The EdU assay confirmed that the downregulation of the first hub gene *CDK1* was correlated to the HCC cell proliferation. Previous study also demonstrated that *CDK1* amplification, observed in 46% of HCC cases, correlates with poor overall survival. In PDX models, combining the *CDK1* inhibitor with sorafenib synergistically suppressed tumor growth and reversed drug resistance by downregulating the *CDK1/PDK1/β-catenin* axis, reducing pluripotency markers and inhibiting epithelial-mesenchymal transition (EMT) [44].

Moreover, disrupted lipid metabolism in the tumor microenvironment impacts immune activity, which in turn drives tumor progression [43, 45]. Thus, the immune signature related to the risk model was also investigated. Based on the TCGA data, Thorsson et al. conducted an in-depth immunogenomic analysis of 33 different cancer types and found six intratumoral immune subtypes, including immunologically quiet, TGF- $\beta$  dominant, inflammatory, lymphocyte depleted, IFN- $\gamma$  dominant, and wound healing [29]. The present study indicated that HCC samples with high RS were enriched in the

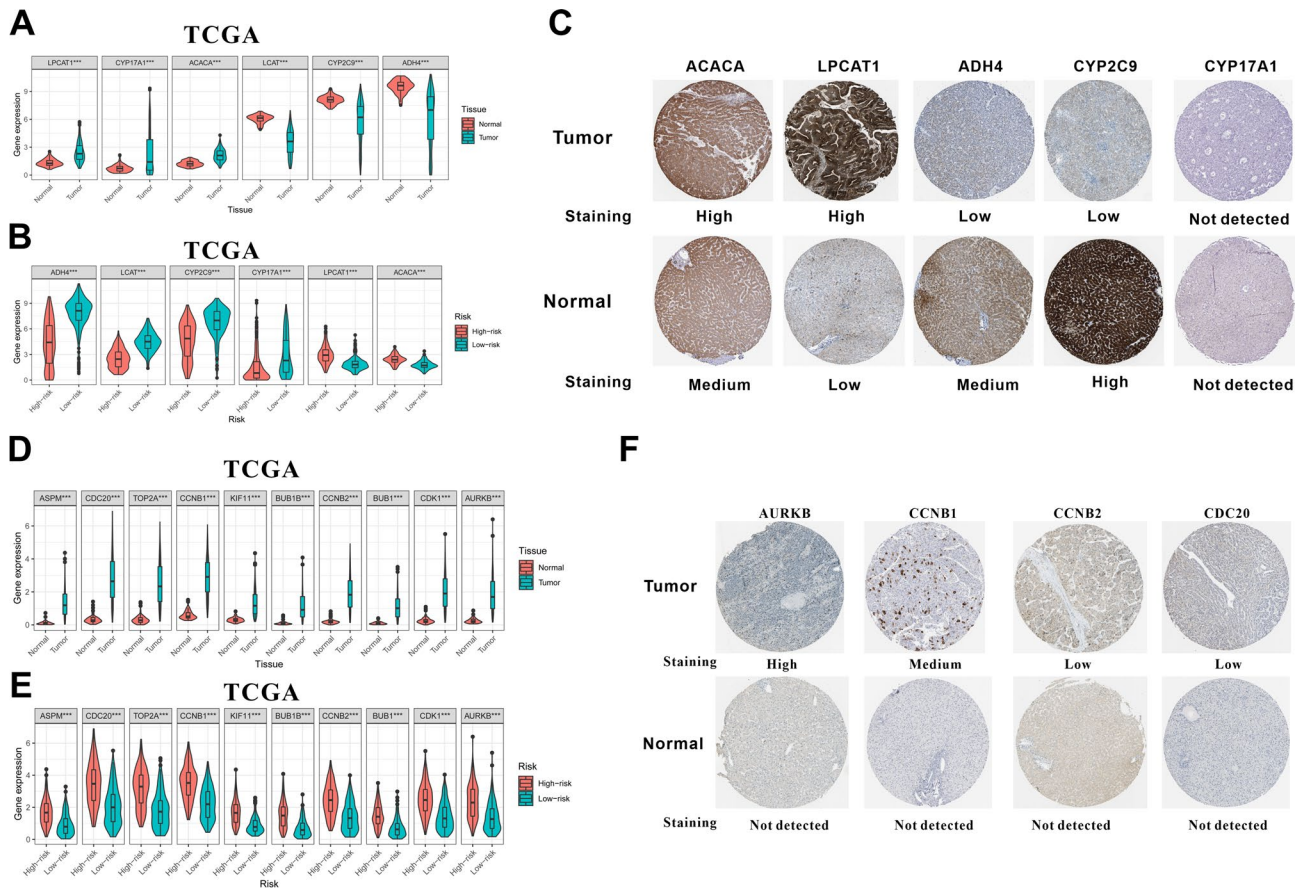


**Fig. 6** Expression of lipid metabolism-related genes and the top ten hub genes. **(A)** mRNA expression of the prognostic genes related to lipid metabolism in normal and tumor tissues in the training group. **(B)** mRNA expression of the prognostic genes related to lipid metabolism in the high- and low-risk groups in the training cohort. **(C)** Immunohistochemical data downloaded from the HPA database demonstrated the protein expression of the prognostic genes related to lipid metabolism in tumor and normal tissues. **(D)** mRNA expression of the top ten hub genes in tumor and normal tissues in the training group. **(E)** mRNA expression of the top ten hub genes in the high- and low-risk groups in the training cohort. **(F)** Immunohistochemical data downloaded from the HPA database demonstrated the protein expression levels of the top ten hub genes between tumor and normal tissues

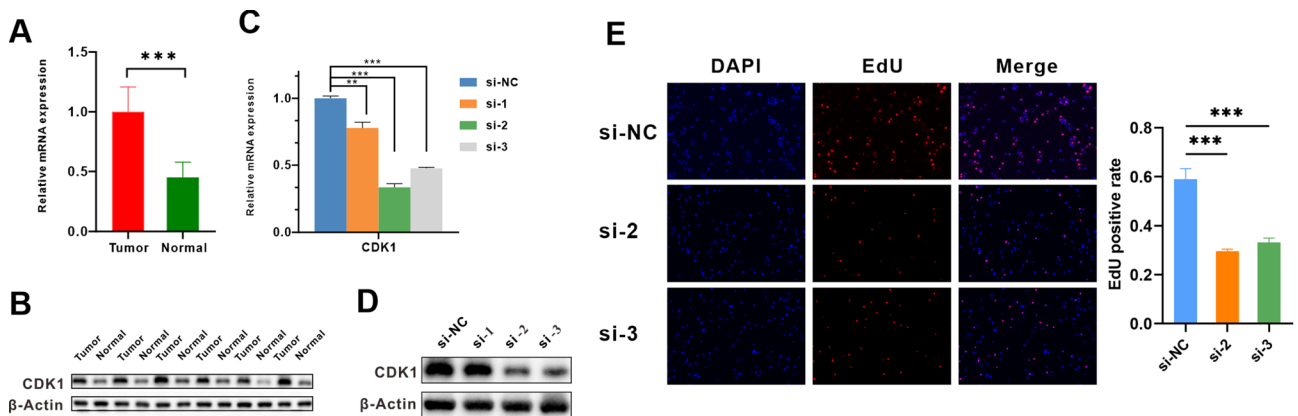


**Fig. 7** Expression and biological functions of the first of the top 10 hub genes *CDK1*. **(A)** qRT-PCR confirmed that *CDK1* was expressed at high levels in tumor samples compared to normal tissue samples. **(B)** Western blotting confirmed that the protein expression of *CDK1* was upregulated in tumor samples. **(C)** mRNA levels in Huh7 cells after *CDK1* knockdown confirmed by qRT-PCR. **(D)** Protein levels in Huh7 cells after *CDK1* knockdown confirmed by western blotting. **(E)** EdU assay showed the decreased proliferation of Huh7 cells after *CDK1* depletion  
 \*\*\*:  $P < 0.001$

wound-healing immune subtype. The wound-healing immune subtype exhibits high proliferation, angiogenic gene expression, and Th2 cell dominance, creating a pro-tumor microenvironment that promotes cancer growth [29, 46]. Meanwhile, the inflammatory immune subtype-enriched HCC patients had low RS. The inflammatory immune subtype characterized by increased *Th1* and *Th17* genes, low proliferation capacity, lower somatic copy number alterations, and aneuploidy indicated an anti-tumor immunity in the tumor microenvironment, which was not conducive to tumor development and progression [29, 47, 48].

Further, the immunocyte subtypes and immune activity were investigated to elucidate the pro-tumor features. CIBERSORT analysis [25, 26] indicated that the high-risk group showed a significantly higher ratio of follicular helper T cells, memory B cells, and neutrophils but a lower average percentage of naïve B cells, M2 macrophages, and  $\gamma\delta$  T cells than the low-risk group. Though the pro-tumor immunocyte subtypes previously mentioned were not detected in the high-risk group, ssGSEA correlation analysis showed weakened cytolytic activity and impaired type I and II IFN response in the high-risk group. Tumor killing is heavily dependent on cytolytic activity [49]. Type I and type II IFN response could directly block the tumor cell cycle progression and induce cell apoptosis as well as simulate anti-tumor immune response and indirectly eliminate tumor cells, thereby preventing metastasis [50, 51]. Thus, the impaired antitumor immune response may be responsible for the pro-tumor immune microenvironment in the high-risk group.

Immunotherapy with checkpoint inhibitors is used as an effective therapeutic strategy as the checkpoint inhibitors have demonstrated potent anti-tumor activity in HCC patients [6, 52, 53]. CTLA-4 and PD1 checkpoint inhibitors, namely, ipilimumab, nivolumab, and pembrolizumab have been approved for advanced HCC treatment by FDA [54]. However, immunotherapies with checkpoint inhibitors do not benefit all HCC patients. The identification of the HCC patients intrinsically resistant to checkpoint inhibitors would help to consider other therapies for HCC, thereby saving a significant sum of financial and medical resources [6, 54].

The present study indicated that the high-risk group expressed ICGs, including HLA (MHC) molecules, CTLA-4, and PD1 at high levels. Rodig et al. confirmed that MHC I downregulation was the primary cause of resistance to anti-CTLA-4 therapy, while MHC II expression was the primary factor contributing to the positive response to anti-PD1 therapy [55]. MHC molecules contribute to the emergence of immunoreactions following inhibitor therapy with checkpoints [54, 56]. In addition, increasing proportions of cells with high expression of

CTLA-4 and PD1 within the tumor-infiltrating CD8+ T cell subset were strongly related to better anti-CTLA4 and anti-PD1 responses. Notably, TIDE analysis identified that our lipid metabolism-related risk model exhibited high predictive value as established biomarkers such as tumor mutational burden (TMB), immune cells and PD-L1 expression in stratifying ICB-responsive HCC patients [57, 58]. While TMB reflects neoantigen load and immune cell or PD-L1 status indicates localized immune activation, our model integrates metabolic dysregulation with immune checkpoint expression, potentially capturing broader mechanisms of therapy resistance. This aligns with recent evidence that lipid metabolism reprogramming directly modulates T cell exhaustion and PD1/CTLA-4 upregulation [59, 60], suggesting a synergistic role of metabolic and immune phenotypes in predicting ICB outcomes. Thus, the lipid metabolism-related gene risk model may be a potential signature for predicting the outcomes in HCC patients treated with anti-CTLA4 and anti-PD1 therapies. Future clinical validation should compare this signature with conventional biomarkers to define its utility in therapeutic decision-making.

Compared to existing lipid metabolism models in HCC, our study offers three key advancements [61, 62]. First, we integrated scRNA-seq data to resolve cell-type-specific lipid metabolic activities, revealing hepatocyte-dominated biosynthesis versus neutrophil-mediated breakdown. This spatial resolution surpasses bulk transcriptome analyses in prior studies. Second, our model uniquely links lipid metabolism to CDK1-driven proliferation, experimentally validated as a therapeutic target, unlike earlier works focused solely on prognostic genes. Third, we incorporated TIDE scoring to predict ICB responsiveness, a feature absent in previous models. Notably, our risk signature achieved higher AUC values (1-year: 0.761 vs. 0.758) [61], underscoring its clinical robustness. These advances position our model as both a prognostic tool and a guide for immunotherapy selection.

Nevertheless, this study has several limitations that should be acknowledged. First, the retrospective design and reliance on public databases may introduce inherent biases, particularly regarding potential confounders in bioinformatics analyses. Factors such as batch effects across different sequencing platforms and tumor heterogeneity within sample cohorts might influence gene expression patterns, potentially affecting the reproducibility and generalizability of our risk model. Second, while our primary focus on RNA-level investigation provides valuable transcriptional insights, this approach cannot fully capture post-transcriptional modifications or protein-level interactions that may critically regulate lipid metabolism pathways. Future studies should employ spatial transcriptomics and single-cell sequencing to address tumor microenvironment complexity, combined

with experimental validation using clinical specimens. Regarding therapeutic translation, our findings suggest potential value in exploring CDK1-targeted strategies and combination therapies that simultaneously modulate lipid metabolism pathways to disrupt cancer progression mechanisms.

#### Abbreviations

AUC	Area under the curve
C-index	Concordance index
DEGs	Differentially expressed genes
EdU	5-Ethynyl-2'-Deoxyuridine
FDA	Food and Drug Administration
GO	Gene Ontology
HCC	Hepatocellular Carcinoma
HPA	Human Protein Atlas
ICB	Immune checkpoint blockade
ICGC	International Cancer Genome Consortium
ICGs	Immune checkpoint genes
KEGG	Kyoto Encyclopedia of Genes and Genomes
OS	Overall survival
PCA	Principal component analysis
PPI	Protein-protein interaction
qRT-PCR	Quantitative real-time PCR
ROC	Receiver operating characteristic
RS	Risk score
scRNA-seq	Single cell RNA sequencing
ssGSEA	Single sample gene set enrichment analysis
TCGA	The Cancer Genome Atlas
TIDE	Tumor immune dysfunction and exclusion

#### Supplementary Information

The online version contains supplementary material available at <https://doi.org/10.1186/s12885-025-14306-6>.

Supplementary Material 1  
 Supplementary Material 2  
 Supplementary Material 3  
 Supplementary Material 4  
 Supplementary Material 5  
 Supplementary Material 6  
 Supplementary Material 7  
 Supplementary Material 8  
 Supplementary Material 9  
 Supplementary Material 10  
 Supplementary Material 11

#### Acknowledgements

The authors sincerely acknowledge the study participants who donated the HCC samples.

#### Author contributions

L. X. and Y. W. conceived the idea, designed the study, analyzed data, performed most of the experiments, and drafted the manuscript. T. X. assisted in data analysis. T.F.C. and H.H.X. supervised the entire project.

#### Funding

The study was supported by the Youth Program of the National Natural Science Foundation of China (No.81902439).

#### Data availability

Data supporting our research can be obtained from public databases or supplemental tables. The datasets generated during the current study are available from the corresponding author on reasonable request.

#### Declarations

##### Ethics approval and consent to participate

This study was performed in accordance with ethical principles that have their origin in the declaration of Helsinki and was approved by the Tongji Hospital Research Ethics Committee. Patients in this study signed informed consent forms independently and agreed to donate tumor tissues and matched paratumor tissues for scientific study.

##### Consent for publication

Not applicable.

##### Competing interests

The authors declare no competing interests.

Received: 25 October 2024 / Accepted: 9 May 2025

Published online: 19 May 2025

#### References

- Forner A, Reig M, Bruix J. Hepatocellular carcinoma. *Lancet*. 2018;391:1301–14. [https://doi.org/10.1016/s0140-6736\(18\)30010-2](https://doi.org/10.1016/s0140-6736(18)30010-2).
- Villanueva A. Hepatocellular Carcinoma. *N Engl J Med*. 2019;380:1450–62. <https://doi.org/10.1056/NEJMra1713263>.
- Bruix J, Qin S, Merle P, Granito A, Huang YH, Bodoky G, Pracht M, Yokosuka O, Rosmorduc O, Breder V, et al. Regorafenib for patients with hepatocellular carcinoma who progressed on Sorafenib treatment (RESORCE): a randomised, double-blind, placebo-controlled, phase 3 trial. *Lancet*. 2017;389:56–66. [https://doi.org/10.1016/S0140-6736\(16\)32453-9](https://doi.org/10.1016/S0140-6736(16)32453-9).
- Cheng AL, Kang YK, Chen Z, Tsao CJ, Qin S, Kim JS, Luo R, Feng J, Ye S, Yang TS, et al. Efficacy and safety of Sorafenib in patients in the Asia-Pacific region with advanced hepatocellular carcinoma: a phase III randomised, double-blind, placebo-controlled trial. *Lancet Oncol*. 2009;10:25–34. [https://doi.org/10.1016/S1470-2045\(08\)70285-7](https://doi.org/10.1016/S1470-2045(08)70285-7).
- Llovet JM, Montal R, Sia D, Finn RS. Molecular therapies and precision medicine for hepatocellular carcinoma. *Nat Rev Clin Oncol*. 2018;15:599–616. <https://doi.org/10.1038/s41571-018-0073-4>.
- Sangro B, Sarobe P, Hervas-Stubb S, Melero I. Advances in immunotherapy for hepatocellular carcinoma. *Nat Rev Gastroenterol Hepatol*. 2021;18:525–43. <https://doi.org/10.1038/s41575-021-00438-0>.
- Llovet JM, Castet F, Heikenwalder M, Maini MK, Mazzaferro V, Pinato DJ, Pikarsky E, Zhu AX, Finn RS. Immunotherapies for hepatocellular carcinoma. *Nat Rev Clin Oncol*. 2022;19:151–72. <https://doi.org/10.1038/s41571-021-00573-2>.
- Palmer DH. Sorafenib in advanced hepatocellular carcinoma. *N Engl J Med*. 2008;359:2498; author reply 2498–2499.
- Kudo M, Finn RS, Qin S, Han KH, Ikeda K, Piscaglia F, Baron A, Park JW, Han G, Jassem J, et al. Lenvatinib versus Sorafenib in first-line treatment of patients with unresectable hepatocellular carcinoma: a randomised phase 3 non-inferiority trial. *Lancet*. 2018;391:1163–73. [https://doi.org/10.1016/S0140-6736\(18\)30207-1](https://doi.org/10.1016/S0140-6736(18)30207-1).
- Abou-Alfa GK, Meyer T, Cheng AL, El-Khoueiry AB, Rimassa L, Ryoo BY, Cicin I, Merle P, Chen Y, Park JW, et al. Cabozantinib in patients with advanced and progressing hepatocellular carcinoma. *N Engl J Med*. 2018;379:54–63. <https://doi.org/10.1056/NEJMoa1717002>.
- Zhu AX, Park JO, Ryoo B-Y, Yen C-J, Poon R, Pastorelli D, Blanc J-F, Chung HC, Baron AD, Pfiffer TEF, et al. Ramucirumab versus placebo as second-line treatment in patients with advanced hepatocellular carcinoma following first-line therapy with Sorafenib (REACH): a randomised, double-blind, multicentre, phase 3 trial. *Lancet Oncol*. 2015;16:859–70. [https://doi.org/10.1016/s1470-2045\(15\)00050-9](https://doi.org/10.1016/s1470-2045(15)00050-9).
- Shlomai A, Leshno M, Goldstein DA. Regorafenib treatment for patients with hepatocellular carcinoma who progressed on sorafenib-A cost-effectiveness analysis. *PLoS ONE*. 2018;13:e0207132. <https://doi.org/10.1371/journal.pone.0207132>.

13. Du D, Liu C, Qin M, Zhang X, Xi T, Yuan S, Hao H, Xiong J. Metabolic dysregulation and emerging therapeutical targets for hepatocellular carcinoma. *Acta Pharm Sin B*. 2022;12:558–80. <https://doi.org/10.1016/j.apsb.2021.09.019>.
14. Degasperis E, Colombo M. Distinctive features of hepatocellular carcinoma in non-alcoholic fatty liver disease. *Lancet Gastroenterol Hepatol*. 2016;1:156–64. [https://doi.org/10.1016/S2468-1253\(16\)30018-8](https://doi.org/10.1016/S2468-1253(16)30018-8).
15. Bian X, Liu R, Meng Y, Xing D, Xu D, Lu Z. Lipid metabolism and cancer. *J Exp Med*. 2021;218. <https://doi.org/10.1084/jem.20201606>.
16. Wang M, Han J, Xing H, Zhang H, Li Z, Liang L, Li C, Dai S, Wu M, Shen F, Yang T. Dysregulated fatty acid metabolism in hepatocellular carcinoma. *Hepat Oncol*. 2016;3:241–51. <https://doi.org/10.2217/hep-2016-0012>.
17. Wu L, Zhang X, Zheng L, Zhao H, Yan G, Zhang Q, Zhou Y, Lei J, Zhang J, Wang J, et al. RIPK3 orchestrates fatty acid metabolism in Tumor-Associated macrophages and hepatocarcinogenesis. *Cancer Immunol Res*. 2020;8:710–21. <https://doi.org/10.1158/2326-6066.CCR-19-0261>.
18. Wang N, Tan HY, Lu Y, Chan YT, Wang D, Guo W, Xu Y, Zhang C, Chen F, Tang G, Feng Y. PIWIL1 governs the crosstalk of cancer cell metabolism and immunosuppressive microenvironment in hepatocellular carcinoma. *Signal Transduct Target Ther*. 2021;6. <https://doi.org/10.1038/s41392-021-00485-8>.
19. Wang MD, Wu H, Fu GB, Zhang HL, Zhou X, Tang L, Dong LW, Qin CJ, Huang S, Zhao LH, et al. Acetyl-coenzyme A carboxylase alpha promotion of glucose-mediated fatty acid synthesis enhances survival of hepatocellular carcinoma in mice and patients. *Hepatology*. 2016;63:1272–86. <https://doi.org/10.1002/hep.28415>.
20. Wang MD, Wu H, Huang S, Zhang HL, Qin CJ, Zhao LH, Fu GB, Zhou X, Wang XM, Tang L, et al. HbX regulates fatty acid oxidation to promote hepatocellular carcinoma survival during metabolic stress. *Oncotarget*. 2016;7:6711–26. <https://doi.org/10.18632/oncotarget.6817>.
21. Chen Y, Pal B, Visvader JE, Smyth GK. Differential methylation analysis of reduced representation bisulfite sequencing experiments using edgeR. *F1000Research*. 2017;6. <https://doi.org/10.12688/f1000research.13196.1>.
22. Longato E, Vettoretti M, Di Camillo B. A practical perspective on the concordance index for the evaluation and selection of prognostic time-to-event models. *J Biomed Inf*. 2020;108:103496. <https://doi.org/10.1016/j.jbi.2020.103496>.
23. Balachandran VP, Gonen M, Smith JJ, DeMatteo RP. Nomograms in oncology: more than Meets the eye. *Lancet Oncol*. 2015;16:e173–80. [https://doi.org/10.1016/S1470-2045\(14\)71116-7](https://doi.org/10.1016/S1470-2045(14)71116-7).
24. Iasonos A, Schrag D, Raj GV, Panageas KS. How to build and interpret a nomogram for cancer prognosis. *J Clin Oncol*. 2008;26:1364–70. <https://doi.org/10.1200/JCO.2007.12.9791>.
25. Chen B, Khodadoust MS, Liu CL, Newman AM, Alizadeh AA. Profiling tumor infiltrating immune cells with CIBERSORT. *Methods Mol Biol*. 2018;1711:243–59. [https://doi.org/10.1007/978-1-4939-7493-1\\_12](https://doi.org/10.1007/978-1-4939-7493-1_12).
26. Newman AM, Liu CL, Green MR, Gentles AJ, Feng W, Xu Y, Hoang CD, Diehn M, Alizadeh AA. Robust enumeration of cell subsets from tissue expression profiles. *Nat Methods*. 2015;12:453–7. <https://doi.org/10.1038/nmeth.3337>.
27. Senbabaoglu Y, Gejman RS, Winer AG, Liu M, Van Allen EM, de Velasco G, Miao D, Ostrovskaya I, Drill E, Luna A, et al. Tumor immune microenvironment characterization in clear cell renal cell carcinoma identifies prognostic and immunotherapeutically relevant messenger RNA signatures. *Genome Biol*. 2016;17. <https://doi.org/10.1186/s13059-016-1092-z>.
28. Jiang P, Gu S, Pan D, Fu J, Sahu A, Hu X, Li Z, Traugh N, Bu X, Li B, et al. Signatures of T cell dysfunction and exclusion predict cancer immunotherapy response. *Nat Med*. 2018;24:1550–8. <https://doi.org/10.1038/s41591-018-0136-1>.
29. Thorsson V, Gibbs DL, Brown SD, Wolf D, Bortone DS, Ou Yang TH, Porta-Pardo E, Gao GF, Plaisier CL, Eddy JA, et al. The immune landscape of Cancer. *Immunity*. 2018;48(e814):812–30. <https://doi.org/10.1016/j.immuni.2018.03.023>.
30. Hu FF, Liu CJ, Liu LL, Zhang Q, Guo AY. Expression profile of immune checkpoint genes and their roles in predicting immunotherapy response. *Brief Bioinform*. 2021;22. <https://doi.org/10.1093/bib/bbaa176>.
31. Hepatocellular carcinoma. *Nat Rev Dis Primers*. 2021;7. <https://doi.org/10.1038/s41572-021-00245-6>.
32. Kulik L, El-Serag HB. Epidemiology and Management of Hepatocellular Carcinoma. *Gastroenterology*. 2019;156:477–491 e471. <https://doi.org/10.1053/j.gastro.2018.08.065>.
33. Chidambaranathan-Reghupaty S, Fisher PB, Sarkar D. Hepatocellular carcinoma (HCC): epidemiology, etiology and molecular classification. *Adv Cancer Res*. 2021;149:1–61. <https://doi.org/10.1016/bs.acr.2020.10.001>.
34. Ackerman D, Simon MC. Hypoxia, lipids, and cancer: surviving the harsh tumor microenvironment. *Trends Cell Biol*. 2014;24:472–8. <https://doi.org/10.1016/j.tcb.2014.06.001>.
35. van Jaarsveld MT, Houthuijzen JM, Voest EE. Molecular mechanisms of target recognition by lipid GPCRs: relevance for cancer. *Oncogene*. 2016;35:4021–35. <https://doi.org/10.1038/ncr.2015.467>.
36. Sangineto M, Villani R, Cavallone F, Romano A, Loizzi D, Serviddio G. Lipid metabolism in development and progression of hepatocellular carcinoma. *Cancers (Basel)*. 2020;12. <https://doi.org/10.3390/cancers12061419>.
37. Butler LM, Perone Y, Dehairs J, Lupien LE, de Laat V, Talebi A, Loda M, Kinlaw WB, Swinnen JV. Lipids and cancer: emerging roles in pathogenesis, diagnosis and therapeutic intervention. *Adv Drug Deliv Rev*. 2020;159:245–93. <https://doi.org/10.1016/j.addr.2020.07.013>.
38. Xu M, Xie P, Liu S, Gao X, Yang S, Hu Z, Zhao Y, Yi Y, Dong Q, Bruns C, et al. LCAT deficiency promotes hepatocellular carcinoma progression and lenvatinib resistance by promoting triglyceride catabolism and fatty acid oxidation. *Cancer Lett*. 2025;612:217469. <https://doi.org/10.1016/j.canlet.2025.217469>.
39. Liu Y, Yu J, An X, Rao H, Qiu Z, Ke J, Wu L, Zhu Z, Deng H, Wu F, et al. TSA attenuates the progression of c-Myc-driven hepatocarcinogenesis by pAKT-ADH4 pathway. *BMC Cancer*. 2024;24:1049. <https://doi.org/10.1186/s12885-024-12781-x>.
40. Peng JY, Cai DK, Zeng RL, Zhang CY, Li GC, Chen SF, Yuan XQ, Peng L. Upregulation of Superenhancer-Driven LncRNA FASRL by USF1 promotes de Novo fatty acid biosynthesis to exacerbate hepatocellular carcinoma. *Adv Sci (Weinh)*. 2022;10:e2204711. <https://doi.org/10.1002/adv.202204711>.
41. Gospodarowicz M, Benedet L, Hutter RV, Fleming I, Henson DE, Sobin LH. History and international developments in cancer staging. *Cancer Prev Control*. 1998;2:262–8.
42. Yao CH, Fowle-Grider R, Mahieu NG, Liu GY, Chen YJ, Wang R, Singh M, Potter GS, Gross RW, Schaefer J, et al. Exogenous fatty acids are the preferred source of membrane lipids in proliferating fibroblasts. *Cell Chem Biol*. 2016;23:483–93. <https://doi.org/10.1016/j.chembiol.2016.03.007>.
43. Yu W, Lei Q, Yang L, Qin G, Liu S, Wang D, Ping Y, Zhang Y. Contradictory roles of lipid metabolism in immune response within the tumor microenvironment. *J Hematol Oncol*. 2021;14:187. <https://doi.org/10.1186/s13045-021-01200-4>.
44. Wu CX, Wang XQ, Chok SH, Man K, Tsang SHY, Chan ACY, Ma KW, Xia W, Cheung TT. Blocking CDK1/PDK1/beta-Catenin signaling by CDK1 inhibitor RO3306 increased the efficacy of Sorafenib treatment by targeting cancer stem cells in a preclinical model of hepatocellular carcinoma. *Theranostics*. 2018;8:3737–50. <https://doi.org/10.7150/thno.25487>.
45. Corn KC, Windham MA, Rafat M. Lipids in the tumor microenvironment: from cancer progression to treatment. *Prog Lipid Res*. 2020;80:101055. <https://doi.org/10.1016/j.plipres.2020.101055>.
46. Cangkruma M, Wietecha M, Werner SW, Repair. Scar formation, and cancer: converging on activin. *Trends Mol Med*. 2020;26:1107–17. <https://doi.org/10.1016/j.molmed.2020.07.009>.
47. Diakos CI, Charles KA, McMillan DC, Clarke SJ. Cancer-related inflammation and treatment effectiveness. *Lancet Oncol*. 2014;15:e493–503. [https://doi.org/10.1016/S1470-2045\(14\)70263-3](https://doi.org/10.1016/S1470-2045(14)70263-3).
48. Coussens LM, Werb Z. Inflammation and cancer. *Nature*. 2002;420:860–7. <https://doi.org/10.1038/nature01322>.
49. Rooney MS, Shukla SA, Wu CJ, Getz G, Hacohen N. Molecular and genetic properties of tumors associated with local immune cytolytic activity. *Cell*. 2015;160:48–61. <https://doi.org/10.1016/j.cell.2014.12.033>.
50. Lazear HM, Schoggins JW, Diamond MS. Shared and distinct functions of type I and type III interferons. *Immunity*. 2019;50:907–23. <https://doi.org/10.1016/j.immuni.2019.03.025>.
51. Jorgovanovic D, Song M, Wang L, Zhang Y. Roles of IFN-gamma in tumor progression and regression: a review. *Biomark Res*. 2020;8:49. <https://doi.org/10.1186/s40364-020-00228-x>.
52. Sangro B, Gomez-Martin C, de la Mata M, Inarrairaegui M, Garralda E, Barrera P, Riezu-Boj J, Larrea E, Alfaro C, Sarobe P, et al. A clinical trial of CTLA-4 Blockade with Tremelimumab in patients with hepatocellular carcinoma and chronic hepatitis C. *J Hepatol*. 2013;59:81–8. <https://doi.org/10.1016/j.jhep.2013.02.022>.
53. El-Khoueiry AB, Sangro B, Yau T, Crocenzi TS, Kudo M, Hsu C, Kim TY, Choo SP, Trojan J, Welling THR, et al. Nivolumab in patients with advanced hepatocellular carcinoma (CheckMate 040): an open-label, non-comparative, phase 1/2 dose escalation and expansion trial. *Lancet*. 2017;389:2492–502. [https://doi.org/10.1016/S0140-6736\(17\)31046-2](https://doi.org/10.1016/S0140-6736(17)31046-2).

54. Bagchi S, Yuan R, Engleman EG. Immune checkpoint inhibitors for the treatment of cancer: clinical impact and mechanisms of response and resistance. *Annu Rev Pathol.* 2021;16:223–49. <https://doi.org/10.1146/annurev-pathol-042020-042741>.
55. Rodig SJ, Gusenleitner D, Jackson DG, Gjini E, Giobbie-Hurder A, Jin C, Chang H, Lovitch SB, Horak C, Weber JS, et al. MHC proteins confer differential sensitivity to CTLA-4 and PD-1 Blockade in untreated metastatic melanoma. *Sci Transl Med.* 2018;10. <https://doi.org/10.1126/scitranslmed.aar3342>.
56. Huang L, Malu S, McKenzie JA, Andrews MC, Talukder AH, Tieu T, Karpinets T, Haymaker C, Forget MA, Williams LJ, et al. The RNA-binding protein MEX3B mediates resistance to Cancer immunotherapy by downregulating HLA-A expression. *Clin Cancer Res.* 2018;24:3366–76. <https://doi.org/10.1158/1078-0432.CCR-17-2483>.
57. Liu Z, Zhang Y, Ma N, Yang Y, Ma Y, Wang F, Wang Y, Wei J, Chen H, Tartarone A, et al. Progenitor-like exhausted SPY1(+)/CD8(+) T cells potentiate responsiveness to neoadjuvant PD-1 Blockade in esophageal squamous cell carcinoma. *Cancer Cell.* 2023;41(e1859):1852–70. <https://doi.org/10.1016/j.ccell.2023.09.11>.
58. Chan TA, Yarchoan M, Jaffee E, Swanton C, Quezada SA, Stenzinger A, Peters S. Development of tumor mutation burden as an immunotherapy biomarker: utility for the oncology clinic. *Ann Oncol.* 2019;30:44–56. <https://doi.org/10.1093/annonc/mdy495>.
59. Wang R, Liu Z, Fan Z, Zhan H. Lipid metabolism reprogramming of CD8(+) T cell and therapeutic implications in cancer. *Cancer Lett.* 2023;567:216267. <https://doi.org/10.1016/j.canlet.2023.216267>.
60. Lim SA, Wei J, Nguyen TM, Shi H, Su W, Palacios G, Dhungana Y, Chapman NM, Long L, Saravia J, et al. Lipid signalling enforces functional specialization of T(reg) cells in tumours. *Nature.* 2021;591:306–11. <https://doi.org/10.1038/s41586-021-03235-6>.
61. Xu K, Xia P, Liu P, Zhang X. A six lipid metabolism related gene signature for predicting the prognosis of hepatocellular carcinoma. *Sci Rep.* 2022;12. <https://doi.org/10.1038/s41598-022-25356-2>.
62. Hao L, Li S, Hu X. Expression of lipid-metabolism genes is correlated with immune microenvironment and predicts prognosis of hepatocellular carcinoma. *Sci Rep.* 2024;14. <https://doi.org/10.1038/s41598-024-76578-5>.

### Publisher's note

Springer Nature remains neutral with regard to jurisdictional claims in published maps and institutional affiliations.